Transportation Research Part C 34 (2013) 148–161

Contents lists available at SciVerse ScienceDirect

Transportation Research Part C

journal homepage: www.elsevier.com/locate/trc

Discontinuities in the Lagrangian formulation of the kinematic wave model

Femke van Wageningen-Kessels [a,*], Yufei Yuan [b], Serge P. Hoogendoorn [a], Hans van Lint [a], Kees Vuik [c]

[a] Delft University of Technology, Faculty of Civil Engineering and Geosciences, Stevinweg 1, Delft, The Netherlands
[b] Delft University of Technology, Faculty of Technology, Policy and Management, Jaffalaan 5, Delft, The Netherlands
[c] Delft University of Technology, Faculty of Electrical Engineering, Mathematics and Computer Science, Mekelweg 4, Delft, The Netherlands

ARTICLE INFO

Article history:
Received 2 August 2010
Received in revised form 18 August 2011
Accepted 22 August 2011

Keywords:
Traffic flow
Continuum models
Networks
Nonhomogeneous roads
Lagrangian formulation
Discretization
Boundaries
Ramps

ABSTRACT

In this article we demonstrate how network components can be modeled using the kinematic wave model in the Lagrangian formulation. This includes modeling nodes (or discontinuities) such as inflow and outflow boundaries, merges and bifurcations (e.g. ramps) and nonhomogeneous roads. Nodes are usually fixed in space. This makes their implementation in Lagrangian coordinates where the coordinates move with the vehicle more complex than in Eulerian coordinates where the coordinates are fixed in space. To this end we derive an analytical node model. The article then discusses how to implement such sink and source terms in a discretized version of the kinematic wave model in Lagrangian coordinates. In this implementation several choices have to be made. Test results show that even with the most simple choices (discretization based on full vehicle groups and discrete time steps) accurate and plausible results are obtained. We conclude that the Lagrangian formulation can successfully be applied for simulation of networks of nonhomogeneous roads.

1. Introduction

Traffic flow models and simulation tools are often used for traffic state estimation and prediction. State estimations are based on data from sensors fixed in space (loop detectors, camera's) and/or on floating car data (gps, mobile phone), which become more popular with the current state of technology. Short term state predictions are used in online applications, for which a low computing time is essential.

In many applications, both for state estimation and prediction, the kinematic wave model by Lighthill and Whitham (1955) and Richards (1956) is used. Recently an alternative formulation of this macroscopic model based on Lagrangian coordinates was introduced by Leclercq et al. (2007). The Lagrangian formulation leads to more efficient simulations than the traditional Eulerian formulation, both in accuracy and computation time (Van Wageningen-Kessels et al., 2010). Furthermore, the Lagrangian formulation results in more efficient traffic state estimation based on floating car data when compared to the Eulerian formulation (Yuan et al., submitted for publication). An other method that can be used to achieve more accurate simulation results is based on variational theory, as introduced for traffic flow by Newell (1993). Daganzo (2005) discusses how this approach can be extended to inhomogeneous roads. However, the variational approach is rather complex to apply on real road networks with many links and when applied to a model with, for example, a non-triangular fundamental diagram, it looses the advantages of higher accuracy. Therefore, in this contribution, we will apply more standard numer-

* Corresponding author. Tel.: +31 (0)15 278 4981; fax: +31 (0)15 278 31 79.
E-mail addresses: f.l.m.vanwageningen-kessels@tudelft.nl (F. van Wageningen-Kessels), y.yuan@tudelft.nl (Y. Yuan), s.p.hoogendoorn@tudelft.nl (S.P. Hoogendoorn), j.w.c.vanlint@tudelft.nl (J.W.C. van Lint), c.vuik@tudelft.nl (C. Vuik).

0968-090X/$ - see front matter
doi:10.1016/j.trc.2011.08.004

ical methods for discretization of the kinematic wave model in Lagrangian formulation. Moreover, the methods we propose here will be better suitable to extend to multi-class models where heterogeneity of drivers and vehicles is taken into account.

For practical (online) applications on real road networks the model has to be completed with boundary conditions. Helbing and Treiber (1999) discuss how to implement boundary conditions in traffic flow models in the Eulerian formulation. Furthermore, models describing flows over nodes, including on- and off-ramps, other merges and bifurcations and inhomogeneities related to (maximum) vehicle speed and number of lanes, have to be included. Such models and their discretization, based on the Eulerian formulation, have been introduced in (Daganzo, 1995; Jin and Zhang, 2003 and Lebacque, 1996). In Jin and Zhang (2003) it is emphasized that at certain inhomogeneities the system of equations is not strictly hyperbolic and numerical diffusion will occur when not properly treated. Laval and Leclercq (2010) discuss a framework to model and analyze congestion at on-ramp bottlenecks. In the Lagrangian formulation, however, implementing boundary conditions and node models is not always straightforward. This is because the coordinates are moving with the vehicles in this formulation, while the boundaries and nodes are fixed in space. It is interesting to note that from a mathematical point of view this problem is very similar to the moving bottleneck problem in Eulerian coordinates, see for example (Leclercq et al., 2004; Newell, 1998). In this article we discuss and demonstrate how to implement in the Lagrangian framework node models and their discretization.

On-ramps and other merges exhibit another difficulty at the onset and presence of congestion and have received much research attention recently. Drivers give each other priority following some fixed merge ratio (Bar-Gera and Ahn, 2010; Cassidy and Ahn, 2005). The merge ratio might be time dependent (e.g. lower in afternoon peak than in morning peak), but it is independent of the actual flows. Many articles have been written on how to implement this merge ratio in a kinematic wave model and its discretization. Laval and Leclercq (2010) develop a method, based on their model in Laval and Leclercq (2008), to analytically find the resulting traffic state at a merge. Since they do not use any numerical approximation, the result is very accurate. However it can only be applied to very simple problems in reasonable computing time. In Eulerian coordinates a merge can be modeled and discretized using, for example the approach described by Ni and Leonard (2005) and Ni et al. (2006). In the latter, modeling and discretization of other network components such as off-ramps is also described. It is based on the simplified theory of kinematic waves (variational theory) by Newell (1993). (Lebacque, 2005) describes several methods for modeling and discretization of merges. One of them was already described by Daganzo (1995) and Lebacque (1996). The discretization approaches are based on the Godunov scheme and therefore, heavily lean on the Eulerian formulation of the kinematic wave model. However, their continuous models turn out to be very useful in describing a merge with priority sharing in the Lagrangian framework. Laval and Leclercq (2008) and Chevallier and Leclercq (2009) describe an approach for merges to be applied in microscopic models. The merge rules formulated in these articles are still rather complex and may contain a stochastic term. Therefore, they are not suitable for a macroscopic model where we do not want to model the behavior of individual vehicles. Instead, we want to model the 'average' vehicle behavior and the discretization should reflect the model as closely as possible. Finally, there are some similarities between modeling nodes in the Lagrangian framework and the treatment of the microscopic to macroscopic boundary and vice versa in hybrid models (Bourrel and Lesort, 2007; Burghout et al., 2005; Laval and Leclercq, 2008; Leclercq, 2007). The methods developed for these models, such as the minimum demand supply scheme in (Leclercq, 2007), can be adapted for our application.

This article presents a complete description of a node model in the Lagrangian formulation of the kinematic wave model (Section 2). The main contribution is a discussion on the discretization of the proposed model. Several methods are discussed in Section 3. Finally we present and discuss simulation results based on the model and its discretization in Section 4.

2. Model

2.1. The basic kinematic wave model

The kinematic wave model for homogeneous roads in Eulerian coordinates consists of the conservation of vehicle equation:

$$\frac{\partial \rho}{\partial t} + \frac{\partial q}{\partial x} = 0, \tag{1}$$

$$\text{with } q = q(\rho) = \rho v(\rho), \tag{2}$$

the equilibrium relation between the flow q (in *vehicle/s*) and the density ρ (in *vehicle/m*). This equilibrium relation is often called the fundamental diagram, which might also refer to the equilibrium relation between vehicle speed v (in m/s) and density. Furthermore, x (in m) and t (in s) are the space and time coordinate, respectively.

The kinematic wave model in Eulerian (t,x) coordinates can be transformed in (t,n) Lagrangian coordinates. Consequently, if n is fixed, x changes over time. The transformation yields the Lagrangian formulation of the kinematic wave model (Leclercq et al., 2007):

$$\frac{\mathrm{D}s}{\mathrm{D}t} + \frac{\partial v}{\partial n} = 0, \tag{3}$$

$$\text{with } \quad \frac{\mathrm{D}}{\mathrm{D}t} = \frac{\partial}{\partial t} + v^{*}(s)\frac{\partial}{\partial x}, \quad \text{the Lagrangian time derivative} \tag{4}$$

$$\text{and} s = 1/\rho, \tag{5}$$

the spacing: the average distance between the tails of two consecutive vehicles in *m*/*vehicle* and *n* the vehicle number. The vehicles are numbered in opposite driving direction: the first vehicle entering the road has the lowest vehicle number. D/D*t* is the partial derivative to time in Lagrangian coordinates, that is: the derivative with respect to time *t* with the other coordinate (vehicle number *n*) fixed. As *n*-coordinates move with vehicle velocity, D*r*/D*t* is the rate of change of some variable *r* as it is observed by a driver moving with velocity $v(n,t) = v(x(n),t) = \partial x/\partial t$. This implies that D/D*t* is a directional derivative in Eulerian coordinates: it is the derivative in the direction of the moving observer (the driver). Both independent variables *t* and *x* change in this direction. The model is completed with the fundamental diagram describing the relation between spacing and vehicle speed:

$$v = v(\rho) = v^*(s). \tag{6}$$

See Fig. 5a for an example of such a fundamental relation.

It turns out that the Lagrangian formulation yields considerable benefits, for instance for numerical simulation (Van Wageningen-Kessels et al., 2010). For practical application of the model, however, complete networks need to be simulated. Therefore, we need to include sources (on-ramps, inflows at entry), sinks (off-ramps, outflow at exit) and other network components such as changes in the number of lanes in the Lagrangian formulation. We use an approach with links and nodes. Links are homogeneous road parts. All links are connected to each other using nodes. Simple nodes have only one ingoing and one outgoing link, and usually represent changes in fundamental diagram parameters (i.e. average drive behavior) due to changes in geometry such as lane-drops (yielding a reduction in capacity) or changes in traffic regulations such as the maximum speed. More complex nodes can have multiple ingoing or outgoing links. In that case the model has to describe how the vehicle flows merge or how the vehicle flows are distributed over the outgoing links.

2.2. Spatio temporal changes in the fundamental diagram

As discussed above a node can represent a change in the fundamental diagram parameters. However, the model described by the conservation Eq. (1) and the fundamental diagram (2), or, equivalently, in Lagrangian coordinates (3) and (6), assumes that the fundamental diagram is constant over space and time. That is, the roads forming the network are homogenous. However, in realistic cases there are many inhomogeneities, for example caused by differences in the number of lanes, speed limits, curves and gradients. This can be incorporated in the model by making the fundamental diagram time and space dependent:

$$q = q(\rho, x, t), \tag{7}$$

or equivalently in Lagrangian formulation:

$$v = v^*(s, x(n), t). \tag{8}$$

2.3. Sink and source terms

To include sinks and sources, we will rewrite the conservation of vehicles equation to include a sink/source term. In Eulerian coordinates we have:

$$\frac{\partial \rho}{\partial t} + \frac{\partial q}{\partial x} = f(x,t). \tag{9}$$

The term $f(x,t) = r(x,t) - s(x,t)$ denotes the time and space dependent source $r(x,t)$ and sink $s(x,t)$ term, usually related to on-ramps or off-ramps. It is important to note that, even though *f* is expressed as the number of vehicles per meter and per second, the source (or sink) is usually located at a point in space. That is, the length of the ramp or the merge region is not taken into account but this length is set to zero. Assuming an infinite long road with a merge at $x = 0$, the source $f(x,t)$ can now be written as:

$$f(x,t) = q_{\text{in}}(0,t)g(x), \tag{10}$$

with $q_{\text{in}}(0,t)$ the inflow from the on-ramp per second. *g* can be any function with $\int_{x=-\infty}^{\infty} g(x)\,dx = 1$. For example, in the following we will use the delta-Dirac function which can loosely be thought of as:

$$g(x) = \delta(x) = \begin{cases} 0 & \text{for} \quad x \neq 0, \\ \infty & \text{for} \quad x = 0, \end{cases} \quad \text{with} \quad \int_{x=-\infty}^{+\infty} \delta(x)\ \mathrm{d}x = 1. \tag{11}$$

(For a rigorous definition of the delta-Dirac function we refer to any calculus or analysis textbook.) Alternatively if one wants to take into account the physical length of the on-ramp $g(x)$ can for example be defined as a block function. We note that the unit of the left-hand side and right-hand side of (10) should be equal and therefore the unit of *g* is chosen to be m^{-1}.

We now first discuss how to reformulate the model with sink or source term in Lagrangian coordinates. Thereafter we will discuss some extra conditions related to priority at merges.

2.3.1. Sink and source terms in the Lagrangian formulation

For the Lagrangian formulation of the node model we use the definitions of spacing (5) and vehicle velocity (6). Combined with the definition of the flow (2) they give:

$$q = v(\rho)\rho = \frac{v^*(s)}{s}. \tag{12}$$

Furthermore, the density can be expressed as the partial derivative of vehicle number n to x:

$$\rho = -\frac{\partial n}{\partial x}, \tag{13}$$

where the minus sign results from the fact that vehicles are numbered in opposite driving direction. From (13) and (5) we find that the partial derivative to x can be rewritten:

$$\frac{\partial}{\partial x} = \frac{\partial}{\partial n}\frac{\partial n}{\partial x} = -\rho\frac{\partial}{\partial n} = -\frac{1}{s}\frac{\partial}{\partial n}. \tag{14}$$

Furthermore, we also need to apply the Lagrangian time derivative (4). Rearrangement and substitution of the partial derivative to x (14) gives:

$$\frac{\partial}{\partial t} = \frac{\mathrm{D}}{\mathrm{D}t} - v^*(s)\frac{\partial}{\partial x} = \frac{\mathrm{D}}{\mathrm{D}t} + \frac{v^*(s)}{s}\frac{\partial}{\partial n}. \tag{15}$$

With the definition of spacing (5) and flow (12) and the Lagrangian derivatives (14) and (15) in hand we can now rewrite the conservation equation including sink and source terms (9) in the Lagrangian framework. To this end we first substitute (5) and (12) into (9), which gives:

$$\frac{\partial(1/s)}{\partial t} + \frac{\partial(v^*(s)/s)}{\partial x} = f(x(n),t). \tag{16}$$

Applying the quotient rule for differentiation and substituting the partial derivatives (14) and (15) gives:

$$-\frac{1}{s^2}\left(\frac{\mathrm{D}s}{\mathrm{D}t} + \frac{v^*(s)}{s}\frac{\partial s}{\partial n}\right) + \frac{1}{s^2}\left(-\frac{\partial v^*(s)}{\partial n} + \frac{v^*(s)}{s}\frac{\partial s}{\partial n}\right) = f(x(n),t). \tag{17}$$

Rearranging and multiplying by $-s^2$ gives our main result:

$$\frac{\mathrm{D}s}{\mathrm{D}t} + \frac{\partial v^*(s)}{\partial n} = -s^2 f(x(n),t). \tag{18}$$

2.3.2. Interpretation of conservation equation with source term

In this section we provide an intuitive interpretation of Eq. (18), especially for the source term on the right-hand side. We will do so on the basis of an alternative *graphical* way to derive the same equation. This graphical explanation is partly based on the derivation of the conservation equation in Lagrangian coordinates *without source term* in (Van Wageningen-Kessels et al., 2010).

In Fig. 1 a t, x plane with some vehicle trajectories is shown. [1] The box is a platoon of vehicles followed over some time Δt. Initially the platoon contains $\Delta n_{\text{initial}}$ vehicles. During the time interval Δt some vehicles (bold arrows) enter the road, e.g. via an on-ramp, and at the end the platoon contains Δn_{end} vehicles. We define the number of vehicles that has entered the platoon:

$$\Delta n_{\text{source}} = \Delta n_{\text{end}} - \Delta n_{\text{initial}}, \quad \Delta n_{\text{end}} = \Delta n_{\text{initial}} + \Delta n_{\text{source}}. \tag{19}$$

The number of vehicles that has entered the platoon is determined by the inflow rate per meter $f(x,t)$, the length of the platoon $s\Delta n \approx s_{\text{initial}}\Delta n_{\text{initial}}$ and the duration Δt:

$$\Delta n_{\text{source}} = f(x(n),t)s_{\text{initial}}\Delta n_{\text{initial}}\Delta t. \tag{20}$$

We note that the source term f has the dimension $(m{\cdot}s)^{-1}$. Therefore, the source is not located at one point in space, but it has a certain length, just as in Eulerian coordinates.

For easy notation from here on we omit the superscript $*$ when denoting the velocity function $v^*(s)$. The length of the platoon at the end $s_{\text{end}}\Delta n_{\text{end}}$ is determined by its initial length $s_{\text{initial}}\Delta n_{\text{initial}}$, the respective distances travelled by the first and the last vehicle in the platoon $v_{\text{first}}\Delta t$ and $v_{\text{last}}\Delta t$:

$$s_{\text{end}}\Delta n_{\text{end}} = s_{\text{initial}}\Delta n_{\text{initial}} + v_{\text{first}}\Delta t - v_{\text{last}}\Delta t. \tag{21}$$

Substituting the number of vehicles from the source (19) and the source term itself (20) gives:

$$(s_{\text{end}} - s_{\text{initial}})\Delta n_{\text{initial}} + (v_{\text{last}} - v_{\text{first}})\Delta t = -s_{\text{end}}f(x(n),t)s_{\text{initial}}\Delta n_{\text{initial}}\Delta t. \tag{22}$$

[1] For interpretation of color in Figs. 1–4, 6–8, the reader is referred to the web version of this article.

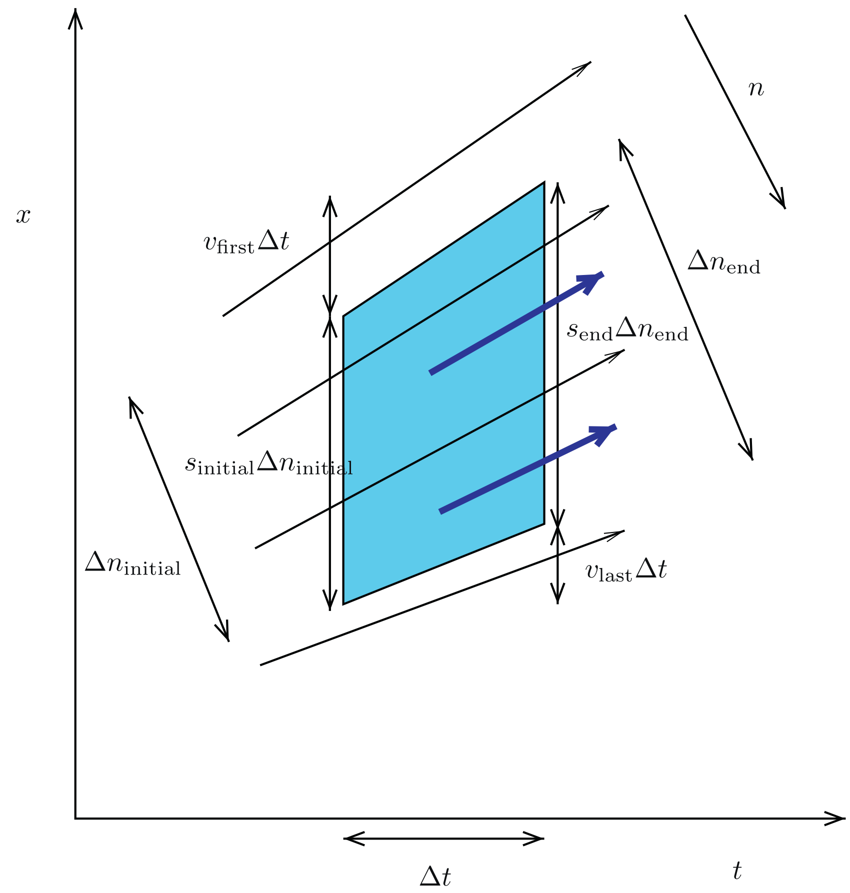

Fig. 1. Graphical interpretation of inhomogeneous kinematic wave model in Lagrangian coordinates. The box is a platoon of vehicles followed over some time Δt. Initially the platoon contains $\Delta n_{\text{initial}}$ vehicles. During the time interval some vehicles (bold arrows) enter the road, e.g. via an on-ramp, and at the end the platoon contains Δn_{end} vehicles.

Rearrangement and dividing both sides by $\Delta n_{\text{initial}}\Delta t$ gives:

$$\frac{s_{\text{end}} - s_{\text{initial}}}{\Delta t} + \frac{v_{\text{last}} - v_{\text{first}}}{\Delta n_{\text{initial}}} = -s_{\text{end}}s_{\text{initial}}f(x(n), t). \tag{23}$$

We assume the platoon is very small ($\Delta n_{\text{initial}} \to 0$), is followed over a short period of time ($\Delta t \to 0$) and $s_{\text{end}}s_{\text{initial}} \to s^2$. Now we can rewrite this as:

$$\frac{\mathrm{D}s}{\mathrm{D}t} + \frac{\partial v}{\partial n} = -s^2 f(x(n), t). \tag{24}$$

The source term on the right-hand side $-s^2f(x(n),t)$ can thus be interpreted as the decrease in platoon length (hence the minus sign) per vehicle and per second due to new platoons of vehicles entering the flow. Of course, in case the source term represents a sink, the net result is an increase in platoon length (spacing) due to platoons of vehicles leaving the flow.

2.4. Bifurcations

Bifurcations are nodes with one incoming and multiple outgoing links. Here we will restrict ourselves to two outgoing links, although the results can easily be generalized. Bifurcations also include off-ramps. At a bifurcation usually a turn fraction is defined. For example, the turn fraction to outgoing link *a* is the fraction of all vehicles arriving at the node that will go to link *a*. These turn fractions can be derived from origin destination matrices, they can be measured directly, or they are for example based on the capacity of the outgoing roads. In this study we assume turn fractions are given. Turn fractions can be used directly in the discretization of the model in Lagrangian coordinates, as we will discuss in the next section.

2.5. Merges

Merges are nodes with multiple incoming and one outgoing links. Here we will restrict ourselves to two incoming links, though the results can easily be generalized. Merges also include on-ramps. In the case of a merge some extra modeling decisions need to be made. They are related to which of the incoming roads gets priority. For example, in reality, vehicles from an on-ramp usually manage to enter the main road relatively easy. When congestion sets in, it spills back onto the main road upstream of the ramp and not (or much less) onto the on-ramp. On the other hand, sometimes a fixed ratio between vehicles from one incoming and vehicles from the other incoming road is observed. These may be the result of specific traffic regulations imposed (priority rules), which are sometimes enforced by geometrical measures (e.g. lane markings). Unless such local priority rules are explicitly known, there are different methods for estimating priority ratios. They are for example based on the capacity of the incoming links or directly on flow measurements. Since we focus on an appropriate macroscopic representation and not on the underlying microscopic drive behavior, in this study we assume the merge priority ratios to be given and we describe how they can be used in modeling a merge in the Lagrangian framework. In Section 3.5 we describe its discretization. The model that we present here is very similar to that proposed by several authors such as Daganzo (1995) and Lebacque (1996, 2005). Let us number the incoming and outgoing links like this:

$$\begin{matrix} 1 \\ 2 \end{matrix} \succ 3.$$

Furthermore, we assume that the merge is located at $x = 0$. The conservation of vehicles tells us that all vehicles that leave either link 1 or 2 will enter link 3. We add a sink/source term to the conservation equations of each incoming or outgoing link l:

$$\frac{\partial \rho_l}{\partial t}(0,t) + \frac{\partial q_l}{\partial x}(0,t) = f_l(0,t). \tag{25}$$

$f_1(0,t)$ and $f_2(0,t)$ are negative and relate to sink terms. Furthermore, $f_3(0,t)$ is positive and relates to a source term:

$$f_3(0,t) = -(f_1(0,t) + f_2(0,t)). \tag{26}$$

Eq. (26) ensures that vehicles are conserved over the merge. We now define the demand D_l as the number of vehicles per second from incoming link l that want to cross the merge:

$$D_l(0^-,t) = \begin{cases} q_l(0^-,t) & \text{if} \quad \rho_l(0^-,t) \leqslant \rho_{\text{crit}}, \\ C_l & \text{otherwise}, \end{cases} \tag{27}$$

with C_l representing the maximum flow (i.e. capacity) in vehicles per second of link l and $0^- = \lim_{\varepsilon \uparrow 0} \varepsilon$ the location just upstream of the merge. Similarly the supply S_l is the number of vehicles per second for which there is still space in outgoing link 3:

$$S_3(0^+,t) = \begin{cases} C_3 & \text{if} \rho_3(0^+,t) \leqslant \rho_{\text{crit}}, \\ q_3(0^+,t) & \text{otherwise}, \end{cases} \tag{28}$$

with $0^+ = \lim_{\varepsilon \downarrow 0} \varepsilon$ the location just downstream of the merge.

Usually, there is no full priority of one incoming link over the other, but a fixed ratio between flows from link 1 and link 2 is observed. Therefore, we define the sink/source at the merge in number of vehicles per second:

$$F_l(0,t) = \int_{x=0^-}^{0^+} f_l(x,t)\,\mathrm{d}x. \tag{29}$$

Assuming that the priority ratio is constant over time we find:

$$\gamma_1 = \frac{F_1(0)}{F_1(0) + F_2(0)} = -\frac{F_1(0)}{F_3(0)}, \quad \text{and} \quad \gamma_2 = \frac{F_2(0)}{F_1(0) + F_2(0)} = -\frac{F_2(0)}{F_3(0)}, \tag{30}$$

The available supply has to be distributed over the incoming links. However, this might lead to under usage of the node. As described before by Daganzo (1995) and Lebacque (1996, 2005) it is most sensible to first distribute the available supply over the links satisfying the ratios. Secondly, if there is still demand from either of the links, this inflow is allowed as long as the total flow over the link does not exceed the downstream supply.

2.6. Boundary conditions

The boundary conditions need to respect inflow restrictions at $x = 0$, and need to enable outflow restrictions at $x = L$. Implementing these in the Lagrangian formulation is straightforward. For the inflow, we have:

$$q(0,t) = \begin{cases} \min(D(t), C), & \text{if}\, \rho(0^+,t) \leqslant \rho_{\text{crit}}, \\ q(0^+,t), & \text{otherwise}, \end{cases} \tag{31}$$

where $D(t)$ denote the traffic demand at time instant t, C denotes the capacity, and ρ_{crit} denotes the critical density (density at capacity). The inflow boundary condition shows that in case of congestion on the road, the inflow is restricted by the flow inside the jam. When conditions are free flow, the inflow is limited by the capacity.

For the outflow, we have:

$$q(L,t) = \begin{cases} \min(\lim_{\varepsilon \downarrow 0} q(L-\varepsilon,t), S(t)), & \text{if } \lim_{\varepsilon \downarrow 0} \rho(L-\varepsilon,t) \leqslant \rho_{cr}, \\ \min(C, S(t)), & \text{otherwise}, \end{cases} \tag{32}$$

where $S(t)$ denotes the outflow restriction at $x = L$ and C is the capacity just upstream of the outflow boundary. The equation allows for restriction of the maximum outflow of a link, e.g. caused by downstream congestion.

3. Discretization

For any simulation or other computer implementation of the model, the model needs to be discretized. Therefore, the vehicles are clustered into groups of Δn vehicles. The vehicle group size $\Delta\, n$ is usually between 1 and 10, but is not necessarily integer. Each vehicle group gets a number i, where the first group that enters the computational domain, has the lowest number. The vehicle discretization is illustrated in Fig. 2. Furthermore, time is discretized into time steps of size Δt, usually between 1 and 8 s. The conservation Eq. (3) is discretized and solved for each time step k. We note that the highest accuracy can be achieved by choosing a small number of vehicles in one group Δn and a small time step size Δt. However, they should always satisfy the CFL-condition (37) to guarantee stable numerical solutions. For a more detailed discussion of the accuracy and convergence of the upwind method with explicit time stepping we refer to (Leclercq et al., 2007).

3.1. Discretization of the basic model

As proposed by Leclercq et al. (2007) the first order upwind method and an explicit time stepping method are used to discretize the conservation equation. For a homogeneous road the conservation Eq. (3) is discretized:

$$s_i^{k+1} = s_i^k + \frac{\Delta t}{\Delta n}\left(v_{i-1}^k - v_i^k\right), \tag{33}$$

with $s_i^k = s(n_i, t^k) = s(n_0 + i\Delta n, t_0 + k\Delta t)$ the spacing associated with the ith vehicle group after k time steps. Furthermore, $v_i^k = v^*(s_i^k)$ is the speed of the ith vehicle group after k time steps, which can be calculated from its spacing using the fundamental diagram.

3.2. Discretization of nodes

In the preceding section, we have shown how inhomogeneities at nodes can be introduced in the Lagrangian formulation of the model. The discretization approach is described in the rest this section.

Therefore, we first discuss the discretization of the model equation with source term (18) in general:

$$s_i^{k+1} = s_i^k + \frac{\Delta t}{\Delta n}\left(v_{i-1}^k - v_i^k\right) + \Delta t \left(s_i^k\right)^2 f(x(n), t). \tag{34}$$

(34) can be rewritten as:

$$s_i^{k+1} = (1+\alpha)s_i^k + \frac{\Delta t}{\Delta n}\left(v_{i-1}^k - v_i^k\right), \tag{35}$$

$$\text{with} \quad \alpha = \Delta t s_i^k f(x(n), t) = \frac{\Delta n^k{}_{\text{source}}}{\Delta n^k_{\text{initial}}}, \tag{36}$$

With $\Delta n_{\text{initial}}$ the total number of vehicles that arrive at the node during the kth time step. In case of a sink, $-\Delta n^k_{\text{source}}$ is the number of vehicles that take the off-ramp during this time step. Now, α relates to the turn fraction, e.g. if $\alpha = -0.2$ this means that 20% of the vehicles just before the ramp take the off-ramp. Similarly, in case of a source, $\Delta n^k_{\text{source}}$ is the number of

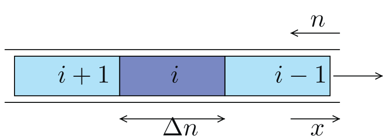

Fig. 2. Vehicle (spatial) discretization of the conservation equation. Driving direction is from left to right. Vehicles and vehicle groups are numbered from right to left.

vehicles that arrive at the node from the on-ramp during this time step and α denotes the number of vehicles added to the flow as a fraction of the flow just before the on-ramp.

Now two issues occur: (1) the number of vehicles in the ith vehicle group changes; (2) if the fundamental diagram $v^*(s)$ changes during the $k+1$th time step, this is not accounted for in the discretization. The first problem is related to the first term on the right-hand side of (35). If α is nonzero the number of vehicles between the $i-1$th and the ith vehicle will change. It can be solved by a proper approach for the vehicle discretization, which will be discussed in Section 3.2.1. The solution to the second issue will be discussed in Section 3.2.2.

3.2.1. Vehicle discretization

The change of the number of vehicles in a vehicle group can give rise to numerical instabilities, particularly if the number of vehicles within one group will become very large. There are two possible approaches to this problem, the first consists of renumbering the vehicles and forming new groups, in the second approach vehicle groups are continued, added to or removed from the flow. The two discretization approaches for a source term describing vehicles merging onto the main road are:

1. All vehicle groups are collected at the source location x where vehicles enter (so both vehicles already on the road and vehicles entering via the source), and new groups are formed. These new groups consist of vehicles from both the main road and the on-ramp or merging road. This approach is illustrated in Fig. 3a.
2. Full vehicle groups are either continued on the main road, and added to the flow at the source location. In other words, the inflow at the source location is added once the total inflow is equal to Δn. This approach is illustrated in Fig. 3b.

The first approach (discontinuing all groups and forming new ones) will lead to more accurate results on a small scale. However, inaccuracies in the latter approach are expected to be small and will, at least partly smooth out due to numerical diffusion. Moreover, the latter approach is easier to program and the calculations can be done faster. In the remaining of this article we will use the simpler approach and discuss its accuracy. For a sink term describing vehicles leaving the main road at a certain location x, similar approaches can be taken, having the same (dis)advantages.

3.2.2. Time discretization

After a vehicle group has reached a boundary or a node some new conditions hold, e.g. the fundamental diagram has changed or vehicles are added to or removed from the vehicle flow. This change usually does not take place at the beginning (or end) of a time step, but during a time step. Therefore, it would be most accurate to let these new conditions apply, also in the discretization, from the moment the node is reached. However, this involves the addition of an extra, intermediate time step, see Fig. 3c. An alternative approach is to let these new conditions apply from the beginning of the next time step, see Fig. 3d. The first approach will lead to more accurate results on a small scale. However, inaccuracies in the latter approach are expected to be small and will, at least partly, decrease over time and space due to numerical diffusion, as described above for vehicle discretization. Moreover, the latter approach is easier to program and the calculations can be done faster. In the remaining of this article we will use the second (less accurate, but simpler) approach.

In the following we will describe the implementation of the above described methods to boundaries and nodes. Therefore, we use the methods where only full vehicle groups are continued, removed from or added to the flow. Furthermore, new conditions after a boundary or node only hold from the beginning of the next time step.

We note that this approach will not lead to vehicle groups overtaking each other. This can be explained by the CFL condition:

$$\frac{\Delta t}{\Delta n}\max\left|\frac{dv}{ds}\right| \leqslant 1. \tag{37}$$

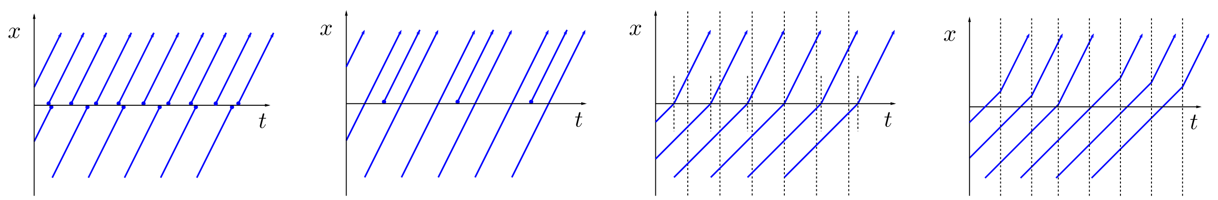

(a) Vehicle discretization for a 2-1 node: all groups are removed, new groups are formed.

(b) Vehicle discretization for a 2-1 node: groups are added to the flow.

(c) Time discretization: new conditions apply from the moment the vehicle group reaches the node.

(d) Time discretization: new conditions apply at the beginning of the first time step after the vehicle groups reached the node.

Fig. 3. Vehicle and time discretization.

The CFL condition (Courant et al., 1967) is a restriction on the discretization that guarantees that a vehicle group i will not, within one time step of size Δt, travel further than the position of the leading vehicle group $i-1$ at the beginning of that time step: $x_i^{k+1} \leqslant x_{i-1}^k$, with x_i^k the position of the ith vehicle group at beginning of the kth time step. This also holds over a node. Moreover, the CFL condition guarantees numerical stability and errors will not grow unbounded.

3.3. Discretization of changes in the fundamental diagram

A spatial or temporal change in the fundamental diagram is for example caused by a change in the speed limit, a spatial change can also be caused by, e.g. a change in the number of lanes. As described before, in the case of a spatial change the new fundamental diagram holds from the beginning of the time step following the time step during which the vehicle group passed the node. Furthermore, in the case of a temporal change in the fundamental diagram, the new conditions apply from the end of the time step after the actual change. In Fig. 4a and b two examples are shown. It can be seen that the change of the fundamental diagram becomes effective in the numerical scheme a bit downstream of the actual change.

3.4. Discretization of 1-2 nodes

A 1-2 node can be an off-ramp or any other bifurcation where one road splits into two. If only the main road is of interest the off-ramp can be seen as a sink, as shown in Fig. 4c. If both outgoing links are included in the network part of the groups go in one direction, the rest of the groups go in the other direction, as shown in Fig. 4d. If furthermore the fundamental diagram changes, this is applied as described before, that is: the new fundamental diagram applies to all groups from the beginning of the next time step after crossing the node. The generalization of this approach to a 1-n node with one incoming and multiple outgoing links is straightforward.

3.5. Discretization of 2-1 nodes

A 2-1 node can be an on-ramp or any other merge where two roads come together and continue as one. If only the state at the main road is important (and the state at the on-ramp or merging road is not important) the approach is as follows. As soon as enough vehicles have arrived at the node, the last vehicle group that passed the node is split into two groups at the beginning of the next time step. Some examples are given in Fig. 4e and f. Fig. 4e shows a merge location where the on-ramp (or other type of incoming link) itself is out of the computational domain. Fig. 4f shows a merge location with the on-ramp (or other type of incoming link) is inside the computational domain and the trajectories of the vehicle groups at that location are shown as broken lines. We note that the groups from the ramp only change there speed from the beginning of the first time step after their arrival at the merge. Sometimes a 2-1 node is combined with a change in the fundamental diagram, for

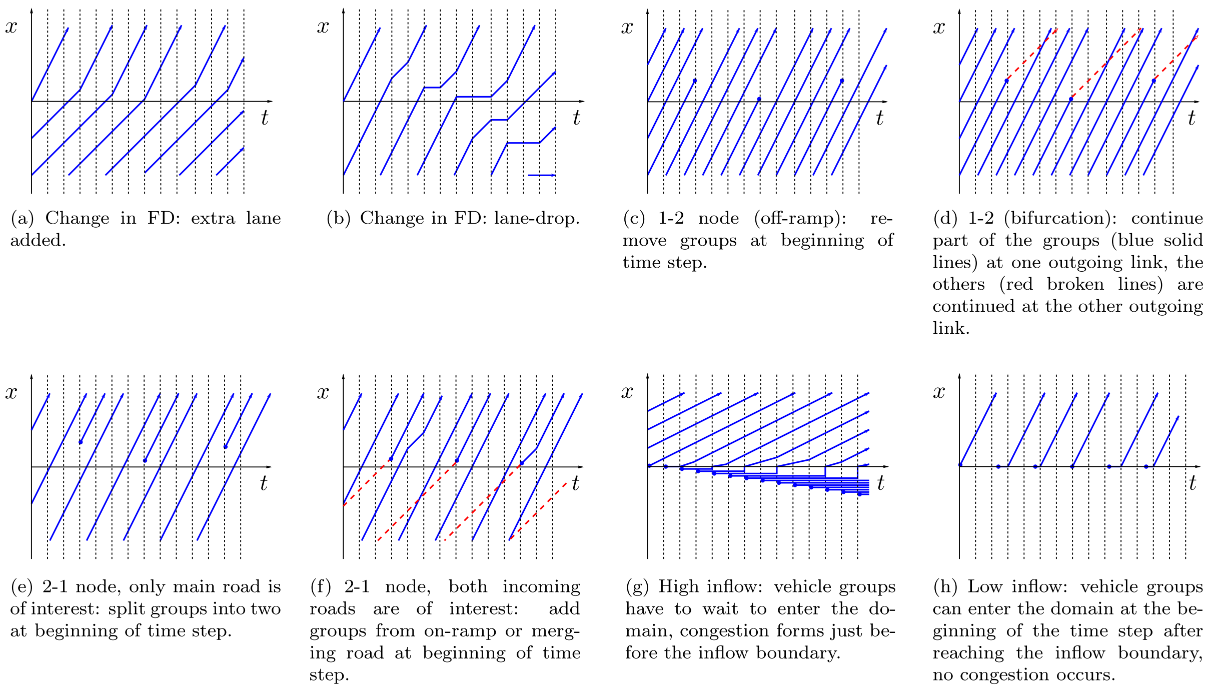

(a) Change in FD: extra lane added.

(b) Change in FD: lane-drop.

(c) 1-2 node (off-ramp): remove groups at beginning of time step.

(d) 1-2 (bifurcation): continue part of the groups (blue solid lines) at one outgoing link, the others (red broken lines) are continued at the other outgoing link.

(e) 2-1 node, only main road is of interest: split groups into two at beginning of time step.

(f) 2-1 node, both incoming roads are of interest: add groups from on-ramp or merging road at beginning of time step.

(g) High inflow: vehicle groups have to wait to enter the domain, congestion forms just before the inflow boundary.

(h) Low inflow: vehicle groups can enter the domain at the beginning of the time step after reaching the inflow boundary, no congestion occurs.

Fig. 4. Discretization of nodes.

example when two two-lane roads are merged and become one three-lane road. If this is the case, the new fundamental diagram is applied just as described before, that is: the new fundamental diagram applies to all groups from the beginning of the next time step after crossing the node. The generalization of this approach to an n-1 node with multiple incoming and one outgoing links is straightforward.

In Section 2.5 we discussed priority rules at merges. The discretization of a $2-1$ merge with priority rules is described below. In the following we assume, without loss of generality that during the $k+1$th time step vehicle group i from link 1 arrives at the merge. First the flow q around the merge has to be calculated. Therefore, (12) is applied to respectively the most downstream vehicle group in link 1 and 2 and the most upstream vehicle group in link 3. Secondly, the discretized priority rules follow from the discussion in Section 2.5. This results in two criteria for a group to pass the node: there must be enough remaining capacity at the outgoing link (that is: the resulting spacing must be lower than critical) and there should be no other group that has priority over this group. Three cases can be distinguished:

1. If only one vehicle group arrives during one time step, it can pass only if the resulting spacing will be higher than critical.
2. If two groups arrive during one time step, calculate M_1 the number of groups from link 1 that recently (within the last M groups) passed the node
   (a) If $M_1 < \gamma_1 M$ the group from link 1 has priority: it can pass, but only if the resulting spacing will be higher than critical.
   (b) If $M_1 \geqslant \gamma_1 M$ the group from link 2 has priority: it can pass, but only if the resulting spacing will be higher than critical.

If one of the groups has passed the node, the other one can also pass but only if the resulting spacing will be higher than critical.

Here M denotes the number of groups that are considered in determining what has recently been the actual merge rate. This M has to be chosen appropriately and can depend on the actual flow rate. However, the tests described in the next section show that it does not really matter whether $M = 1$, $M = 5$ or $M = 10$. The discretization above can roughly be interpreted as follows: all arriving vehicles can pass the merge immediately, except if there are too many vehicles at or around the merge. In that case the vehicles pass according to some predefined merge ratio.

3.6. Discretization of the boundary conditions

At an inflow boundary ($x = 0$), the arriving flow, that is the number of vehicles per time unit that arrive at the inflow boundary is prescribed as in (31). The numerical discretization of the inflow boundary is shown schematically in Fig. 4g and h. It comes down to releasing a vehicle group of size Δn to enter the computational domain at the beginning of a time step whenever enough vehicles have arrived. We note that if there is congestion downstream of the inflow boundary or if the inflow is larger than the maximum road capacity this might mean that one or more vehicle groups are waiting at the inflow boundary until they can enter, as is shown in Fig. 4g. Furthermore, even if there is enough space directly after the arrival of vehicles forming a new vehicle group, the group has to wait until the beginning of the next time step to enter the domain. This leads to a delay of one group of at most the time step size Δt, see Fig. 4h.

At the outflow boundary ($x = L$) the mixed boundary condition (32) is used. Therefore, the flow just before the boundary, that is the flow related to the last vehicle group that has left the domain needs to be calculated:

$$q(L^-, t) = q(x(0), t) = \frac{v^*(0,t)}{s(0,t)}, \tag{38}$$

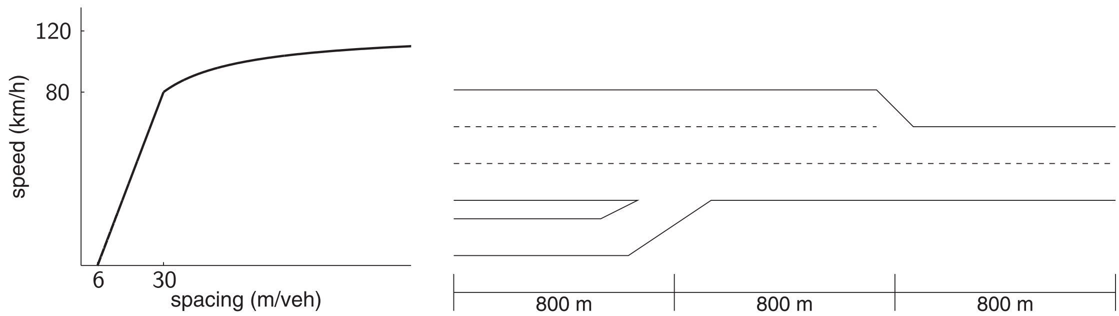

(a) Smulders fundamental diagram (per lane). In free flow (right part) the density-speed relationship is linear, in congestion (left part) the spacing-speed relationship is linear.

(b) Road layout with merge and lane-drop.

Fig. 5. Fundamental diagram and road layout of test case.

Table 1
Parameter settings for simulation.

Free flow speed	120 km/h
Critical speed	80 km/h
Critical spacing per lane	30 m/veh
Minimum spacing per lane	6 m/veh
Inflow main road	0.6× or 8× capacity veh/h
Inflow on-ramp	0.6× or 0.8× capacity veh/h
Vehicle group size	10 or 2 veh
Time step size	3.2 or 0.64 s
Nr of vehicle groups for merge priority (M)	5 or 1

where $L^- = \lim_{\varepsilon \uparrow 0} L - \varepsilon$ the location just upstream of the outflow boundary and $x(0)$ denotes the location of the last vehicle group (group $n = 0$) that has left the domain. If the flow of group 0 is lower than the outflow restriction $S(t)$ all vehicle groups are allowed to leave the domain and no special procedure is needed for discretization. If, however, the flow of group 0 is higher than the outflow restriction not all vehicle groups are allowed to leave the domain and congestion will spill back into the domain. Again, no special procedure is needed for the discretization of the boundary condition.

4. Simulations and results

The above described method combined with the fundamental diagram in Fig. 5a was applied to a main road with an on-ramp. Two kilometer after the merge the number of lanes of the main road drops from 3 to 2, see Fig. 5b. The parameters in Table 1 were used. With these parameter settings the CFL-condition (37) is satisfied as an inequality: $(\Delta t/\Delta n)\max|\mathrm{d}v/\mathrm{d}s| = 8/9$. For the outflow boundary no restriction was applied. Three cases were studied:

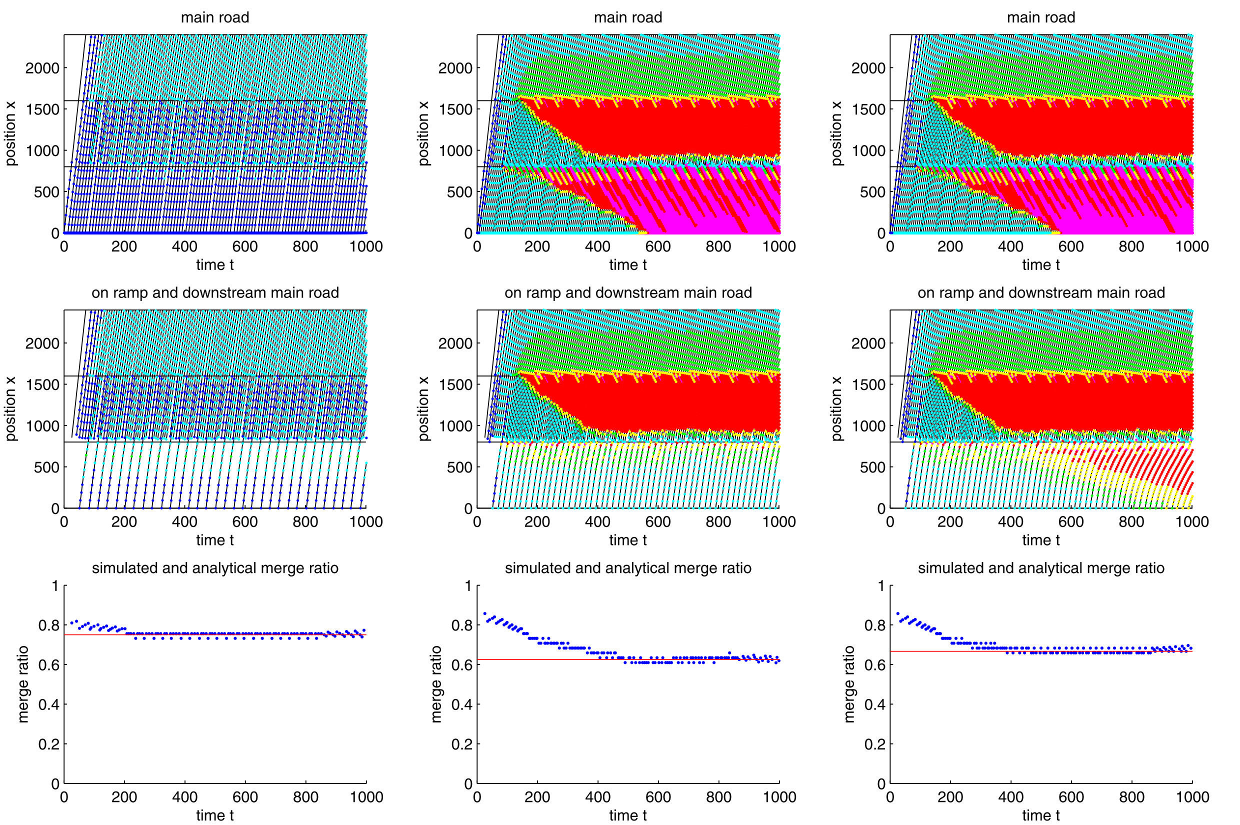

(a) Case 1: low inflow.
(b) Case 2: high inflow, full priority for on-ramp.
(c) Case 3: high inflow, main road 'some' priority over on-ramp.

Fig. 6. Results of on-ramp bottleneck simulations. Top: trajectories (black lines) of vehicles on main road. Center: trajectories (black lines) of vehicles on on-ramp and on main road downstream of on-ramp. Colored dots indicate local vehicle speed: ● magenta: $v < 0.2v_{crit}$, ● red: $0.2v_{crit} \leqslant v < 0.4v_{crit}$, ● yellow: $0.4v_{crit} \leqslant v < 0.7v_{crit}$, ● green: $0.7\ v_{crit} \leqslant v < v_{crit}$, ● cyan: $v_{crit} \leqslant v < 0.5\ (v_{crit} + v_{max})$, ● blue: $0.5(v_{crit} + v_{max}) \leqslant v < v_{max}$. Bottom: resulting merge ratio (dots) and expected merge ratio (line).

1. Low inflow: at inflow boundary of main road: 0.45× capacity of main road downstream of merge location, at on-ramp: 0.15× capacity of main road downstream of merge location.
2. High inflow: at inflow boundary of main road: 0.6× capacity of main road downstream of merge location, at on-ramp: 0.2× capacity of main road downstream of merge location. And full priority for on-ramp ($\gamma_{\text{main road}} = 0$, $\gamma_{\text{on-ramp}} = 1$).
3. High inflow: as case 2 but with merge priority ($\gamma_{\text{main road}} = 2/3$, $\gamma_{\text{on-ramp}} = 1/3$).

The results can be seen in Fig. 6.

Furthermore, we studied the influence of the number of vehicle groups that were used in determining merge priority and the influence of the numerical resolution (vehicle group size and time step size). The results of case 2 (with normal resolution) and only the last vehicle group determining the priority ($M = 1$ instead of $M = 5$) are shown in Fig. 7a. The results of case 2 with small vehicle groups, small time steps and thus a high resolution ($\Delta n = 2$, $\Delta t = 0.64$ s instead of $\Delta n = 10$, $\Delta t = 3.2$ s) are shown in Fig. 7b.

4.1. Discussion of simulation results

From the results of case 1 (Fig. 6a) we see that with low inflow no congestion occurs, as is to be expected. Furthermore, the simulated merge ratio only depends on the inflow rates and there is no influence of the merge priority (not shown). From the results of case 2 and 3 (Fig. 6b and c) we see that congestion starts at the bottleneck caused by this lane-drop. It then spills back to the merge. There is also a little congestion at the main road starting at the merge. This is not supposed to occur since the total inflow is equal to the capacity downstream of the node. This congestion is due to the discretization method. Other tests (results not shown) show that this only occurs when the total inflow from main road and on-ramp is at or just below capacity of the main road. A possible remedy can be found in applying a more exact procedure for both vehicle and time discretization, as described in Sections 3.2.1, 3.2.2.

Finally, when the congestion from the lane-drop spills back to the merge the influence of the merge priority can be observed. In case 2 (full priority for the on-ramp), the on-ramp remains in free flow, while the main road upstream of the merge

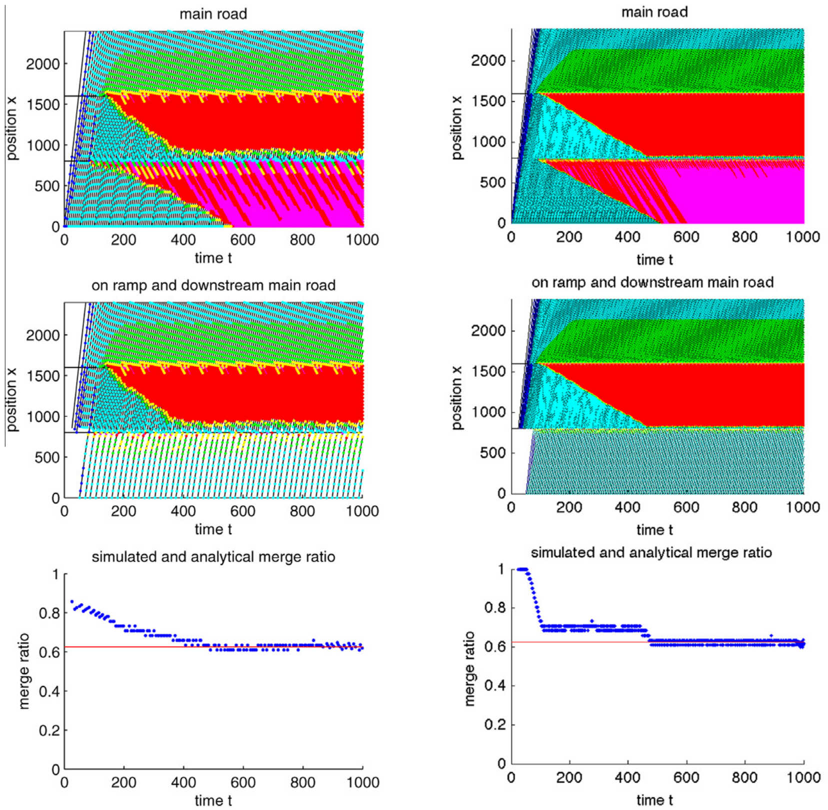

(a) Results of an on-ramp bottleneck simulation, case 2 with a low number of vehicles to determine priority ($M = 1$ instead of $M = 5$).

(b) Results of an on-ramp bottleneck simulation, case 2 with a high resolution ($\Delta n = 2$ instead of $\Delta n = 10$).

Fig. 7. Results of on-ramp bottleneck simulations, with some adjusted numerical parameters. Legend: see Fig. 6.

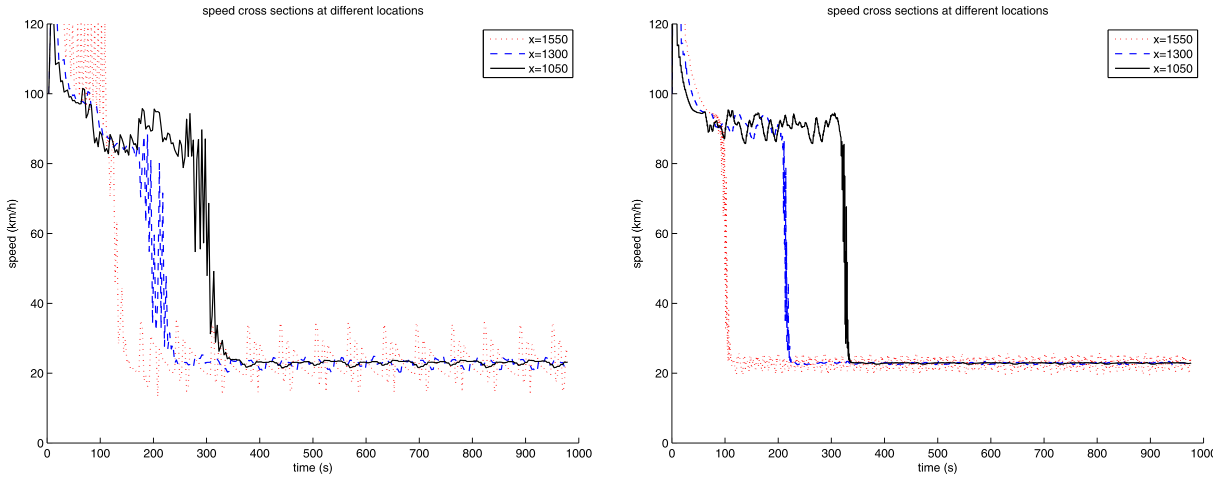

(a) Low resolution. (b) High resolution ($\Delta n = 2$ instead of $\Delta n = 10$).

Fig. 8. Vehicle speeds in case 2 at three cross sections of the main road between the on-ramp and the lane-drop.

becomes (more) congested. In case 3, where the priority is distributed over both incoming links, also the congestion spills back over both incoming links. The calculated merge ratio is, in the long run, as expected from the analytical results.

The influence of the number of vehicle groups to determine the priority (M) was tested only for case 2. The results (see Fig. 7a) show that the influence is negligible. We have also tested this with $M = 10$ (not shown), again the results were similar. Case 2 was also used to study the influence of the numerical resolution (see Fig. 7b). Both the vehicle group size and time step size were taken five times as small. The overall results are similar. However, in the low resolution case 'artificial stop-and-go waves' can be observed. Small low speed regions are created at the bottleneck and travel upstream. In the high resolution case, they have disappeared almost completely. In other simulation results (not shown) we have found that when the CFL-condition is satisfied as an equality, there is less numerical diffusion and the artificial waves do not disappear. The diffusion of the disturbances is also illustrated in Fig. 8. It shows that the artificial stop-and-go waves are indeed due to the numerical discretization and resolution. Moreover, these artificial waves only influence a small region and they disappear almost completely due to diffusion, in the low resolution case within 550 m upstream, in the high resolution case even within 300 m upstream.

5. Conclusion

In this article we have derived an analytical expression for network components such as sinks and sources, boundaries and changes in the fundamental diagram in the Lagrangian formulation of the kinematic wave model. The formulation clearly shows how nodes in Lagrangian coordinates effectively generate (or remove) vehicles into (from) the flow and as a result change the spacing of vehicles that pass the node.

In the discretized case we find that there are several options to choose from in terms of vehicle discretization and time discretization. At the nodes, one can either break up all groups and form new ones according to the amount of vehicles entering or leaving or one could maintain the existing vehicle groups and add or remove group (in units Δn) entering or exiting. Although the first method will lead to more accurate results on a small scale, the second method is more easy to implement and leads to plausible and accurate results. A similar design choice relates to time discretization. One could add vehicles at the time a group first passes the node, or do this at the next time step. Again the first option will lead to more accurate results, whereas the second is more straightforward to implement and leads to plausible and accurate results.

A disadvantage of the numerical solution method is the introduction of artificial stop-and-go waves and congestion. We have shown that they are indeed created by the numerical method and that the stop-and-go-waves diffuse quickly. However, they can easily be misinterpreted as real stop-and-go waves. More exact approaches, such as the other choices we mentioned or an approach based on the minimum supply and demand scheme to be applied only at the nodes will lead to more accurate results, without artificial stop-and-go waves. Furthermore, at inhomogeneities such as changes in the fundamental diagram the conservation Eq. (1) or equivalently (3) is not strictly hyperbolic. Therefore, the proposed numerical method will create numerical diffusion. This might be prevented by applying methods such as proposed in (Jin and Zhang, 2003).

Models of boundaries and nodes make it possible to model networks consisting of many interconnected inhomogeneous roads in Lagrangian coordinates. These models and corresponding simulation tools and can be applied for online traffic state estimation and prediction on real freeway networks. The computations based on the Lagrangian formulation are more efficient (both in computation time and accuracy) than computations based on the Eulerian formulation. This has been verified for traffic state estimation in (Yuan et al., 2011). Furthermore, these 'building blocks' of a network are necessary for evaluation of the model based on traffic data from either sensors fixed in space or floating car data.

With a reliable means at hand to implement nodes into the Lagrangian framework, larger scale modeling of traffic networks on the basis of the Lagrangian formulation becomes possible. Further research efforts will focus on such network implementations. Secondly, the mixed-class node models and their discretization developed here will be generalized for application to multi-class kinematic wave models. Furthermore, more exact approaches such as described above will be studied, as well as errors introduced by the proposed methods.

Acknowledgements

The authors would like to thank the anonymous reviewers. Femke van Wageningen-Kessels is a PhD-student at the ITS Edulab, a collaboration between TUDelft and Rijkswaterstaat and a member of TRAIL Research School.

References

Bar-Gera, H., Ahn, S., 2010. Empirical macroscopic evaluation of freeway merge-ratios. Transportation Research Part C: Emerging Technologies 18 (4), 457–470.

Bourrel, E., Lesort, J.-B., 2007. Mixing microscopic and macroscopic representations of traffic flow hybrid model based on Lighthill–Whitham–Richards theory. Transportation Research Record: Journal of the Transportation Research Board 1852, 193–200.

Burghout, W., Koutsopoulos, H., Andréasson, I., 2005. Hybrid mesoscopic–microscopic traffic simulation. Transportation Research Record: Journal of the Transportation Research Board 1934, 218–225.

Cassidy, M., Ahn, S., 2005. Driver turn-taking behavior in congested freeway merges. Transportation Research Record: Journal of the Transportation Research Board 1934, 140–147.

Chevallier, E., Leclercq, L., 2009. Do microscopic merging models reproduce the observed priority sharing ratio in congestion? Transportation Research Part C: Emerging Technologies 17 (3), 328–336.

Courant, R., Friedrichs, K., Lewy, H., 1967. On the partial difference equations of mathematical physics. IBM Journal, 215–234.

Daganzo, C., 2005. A variational formulation of kinematic waves: I. Basic theory and complex boundary conditions and II. Solution methods. Transportation Research Part B 39, 187–196 (934–950).

Daganzo, C.F., 1995. The cell transmission model, part II: Network traffic. Transportation Research Part B: Methodological 29 (2), 79–93.

Helbing, D., Treiber, M., 1999. Numerical simulation of macroscopic traffic equations. Computing in Science and Engineering 1 (5), 89–99.

Jin, W.-L., Zhang, H.M., 2003. The inhomogeneous kinematic wave traffic flow model as a resonant nonlinear system. Transportation Science 37 (3), 294–311.

Laval, J., Leclercq, L., 2010. Continuum approximation for congestion dynamics along freeway corridors. Transportation Science 40 (1), 87–97.

Laval, J.A., Leclercq, L., 2008. Microscopic modeling of the relaxation phenomenon using a macroscopic lane-changing model. Transportation Research Part B: Methodological 42 (6), 511–522.

Lebacque, J., 1996. The Godunov scheme and what it means for first order traffic flow models. In: Lesort, J. (Ed.), Transportation and Traffic Theory. Pergamon, pp. 647–677.

Lebacque, J., 2005. Intersection modeling, application to macroscopic network traffic flow models and traffic management. In: Hoogendoorn, S.P., Luding, S., Bovy, P.H.L., Schreckenberg, M., Wolf, D.E. (Eds.), Traffic and Granular Flow, vol. 03. Springer, Berlin, Heidelberg, pp. 261–278.

Leclercq, L., 2007. Hybrid approaches to the solutions of the Lighthill–Whitham–Richards" models. Transportation Research Part B: Methodological 41 (7), 701–709.

Leclercq, L., Chanut, S., Lesort, J.-B., 2004. Moving bottlenecks in Lighthill–Whitham–Richards model: a unified theory. Transportation Research Record: Journal of the Transportation Research Board 1883, 3–13.

Leclercq, L., Laval, J., Chevallier, E., 2007. The Lagrangian coordinates and what it means for first order traffic flow models. In: Allsop, R., Bell, M., Heydecker, B. (Eds.), Transportation and Traffic Theory. Elsevier, Oxford, UK, pp. 735–753.

Lighthill, M.J., Whitham, G.B., 1955. On kinematic waves. II. A theory of traffic flow on long crowded roads. Proceedings of the Royal Society of London. Series A, Mathematical and Physical Sciences 229 (1178), 317–345.

Newell, G., 1993. A simplified theory of kinematic waves in highway traffic (part I–III). Transportation Research Part B: Methodological 27 (4), 281–313.

Newell, G.F., 1998. A moving bottleneck. Transportation Research Part B: Methodological 32 (8), 531–537.

Ni, D., Leonard II, J., 2005. A simplified kinematic wave model at a merge bottleneck. Applied Mathematical Modelling 29 (11), 1054–1072.

Ni, D., Leonard II, J., Williams, B., 2006. The network kinematic waves model: a simplified approach to network traffic. Journal of Intelligent Transportation Systems: Technology, Planning, and Operations 10, 1–14.

Richards, P.I., 1956. Shock waves on the highway. Operations Research 4 (1), 42–51.

Van Wageningen-Kessels, F., Van Lint, J., Hoogendoorn, S., Vuik, C., 2010. Lagrangian formulation of a multi-class kinematic wave model. Transportation Research Record: Journal of the Transportation Research Board 2188, 29–36.

Yuan, Y., Van Lint, H., van Wageningen-Kessels, F., Hoogendoorn, S., 2011. Lagrangian traffic state estimation for freeway networks. In: 2nd International Conference on Models and Technologies for ITS.

Yuan, Y., Van Lint, J., Wilson, R., van Wageningen-Kessels, F., Hoogendoorn, S., submitted for publication. Real-time lagrangian traffic state estimator for freeways. IEEE ITS Transactions.